

Heterodimerization of Dibenzodiazepinone-Type Muscarinic Acetylcholine Receptor Ligands Leads to Increased M₂R Affinity and Selectivity

Xueke She,^{†,§} Andrea Pegoli,[†] Judith Mayr,^{†,||} Harald Hübner,[‡] Günther Bernhardt,[†] Peter Gmeiner,^{‡,ID} and Max Keller^{*,†,ID}

[†]Institute of Pharmacy, Faculty of Chemistry and Pharmacy, University of Regensburg, Universitätsstr. 31, D-93053 Regensburg, Germany

[‡]Department of Chemistry and Pharmacy, Emil Fischer Center, Friedrich Alexander University, Schuhstr. 19, D-91052 Erlangen, Germany

S Supporting Information

ABSTRACT: In search for selective ligands for the muscarinic acetylcholine receptor (MR) subtype M₂, the dimeric ligand approach, that is combining two pharmacophores in one and the same molecule, was pursued. Different types (agonists, antagonists, orthosteric, and allosteric) of monomeric MR ligands were combined by various linkers with a dibenzodiazepinone-type MR antagonist, affording five types of heterodimeric compounds (“DIBA-xanomeline,” “DIBA-TBPB,” “DIBA-77-LH-28-1,” “DIBA-propantheline,” and “DIBA-4-DAMP”), which showed high M₂R affinities (pK_i > 8.3). The heterodimeric ligand UR-SK75 (**46**) exhibited the highest M₂R affinity and selectivity [pK_i (M₁R–M₃R): 8.84, 10.14, 7.88, 8.59, and 7.47]. Two tritium-labeled dimeric derivatives (“DIBA-xanomeline”-type: [³H]UR-SK71 ([³H]**44**) and “DIBA-TBPB”-type: [³H]UR-SK59 ([³H]**64**)) were prepared to investigate their binding modes at hM₂R. Saturation-binding experiments showed that these compounds address the orthosteric binding site of the M₂R. The investigation of the effect of various allosteric MR modulators [gallamine (**13**), W84 (**14**), and LY2119620 (**15**)] on the equilibrium (**13**–**15**) or saturation (**14**) binding of [³H]**64** suggested a competitive mechanism between [³H]**64** and the investigated allosteric ligands, and consequently a dualsteric binding mode of **64** at the M₂R.

homodimeric ligand		x	pK _i hM ₂ R
		1	9.00
		2	9.51
		3	8.17
		4	8.97
		5	7.64

↓ increase in M₂R selectivity

heterodimeric ligand		x	pK _i hM ₂ R
		1	8.84
		2	10.14
		3	7.88
		4	8.59
		5	7.47

1. INTRODUCTION

Muscarinic acetylcholine receptors (MRs) belong to the class A G-protein coupled receptor (GPCR) superfamily and comprise five receptor subtypes in humans (designated M₁R–M₅R).^{1–4} Whereas the M₁R, M₃R, and M₅R receptors were reported to couple with G_q proteins, the M₂R and M₄R receptors bind to G_{i/o} proteins.⁵ MRs represent interesting drug targets, for instance, for the treatment of Alzheimer’s disease and schizophrenia.^{6,7} Because of the high conservation of the orthosteric (acetylcholine) binding site,^{8–10} there is lack of highly subtype selective (orthosteric) ligands, hampering therapeutic approaches such as the treatment of cognitive decline by centrally acting selective M₁R agonists or M₂R antagonists.¹¹ However, in addition to the orthosteric binding pocket, MRs were reported to exhibit distinct allosteric binding sites, which are less conserved and can potentially be exploited to develop subtype selective ligands.^{12–17} The M₂R was the first GPCR described to be subjected to allosteric modulation,^{18–20} and several dualsteric M₂R ligands (e.g., **7**,²¹ and **10**,^{22,23} Figure 1A) and allosteric M₂R modulators (e.g., **13**,²⁰ **14**,¹⁸ and **15**,^{24,25} Figure 1B) were identified.

Dimerization of GPCR ligands can result in an increased receptor affinity and improved selectivity.^{26,27} Bivalent (dimeric) ligands were described for various GPCRs, such as opioid,²⁸ histamine,^{29,30} dopamine,^{31–33} adenosine,^{33–35} and neuropeptide Y^{36–38} receptors, not least to investigate receptor dimerization. Likewise, the design of dualsteric (bitopic) ligands, that is, hybrid derivatives that simultaneously address the orthosteric and allosteric sites of one and the same receptor protomer, represents an approach toward improved subtype selectivity.^{19,39–42} For example, rationally designed hybrid MR ligands derived from the orthosteric agonist oxotremorine (**2**) and hexamethonium-like allosteric modulators (e.g., compound **16**, Figure 1C) showed increased subtype selectivity compared to **2**.⁴³ Similarly, the MR ligand THRX-160209 (compound **17**, Figure 1C) was reported to exhibit a higher M₂R affinity and selectivity than the corresponding monovalent ligands and

Received: July 28, 2017

Accepted: September 5, 2017

Published: October 16, 2017

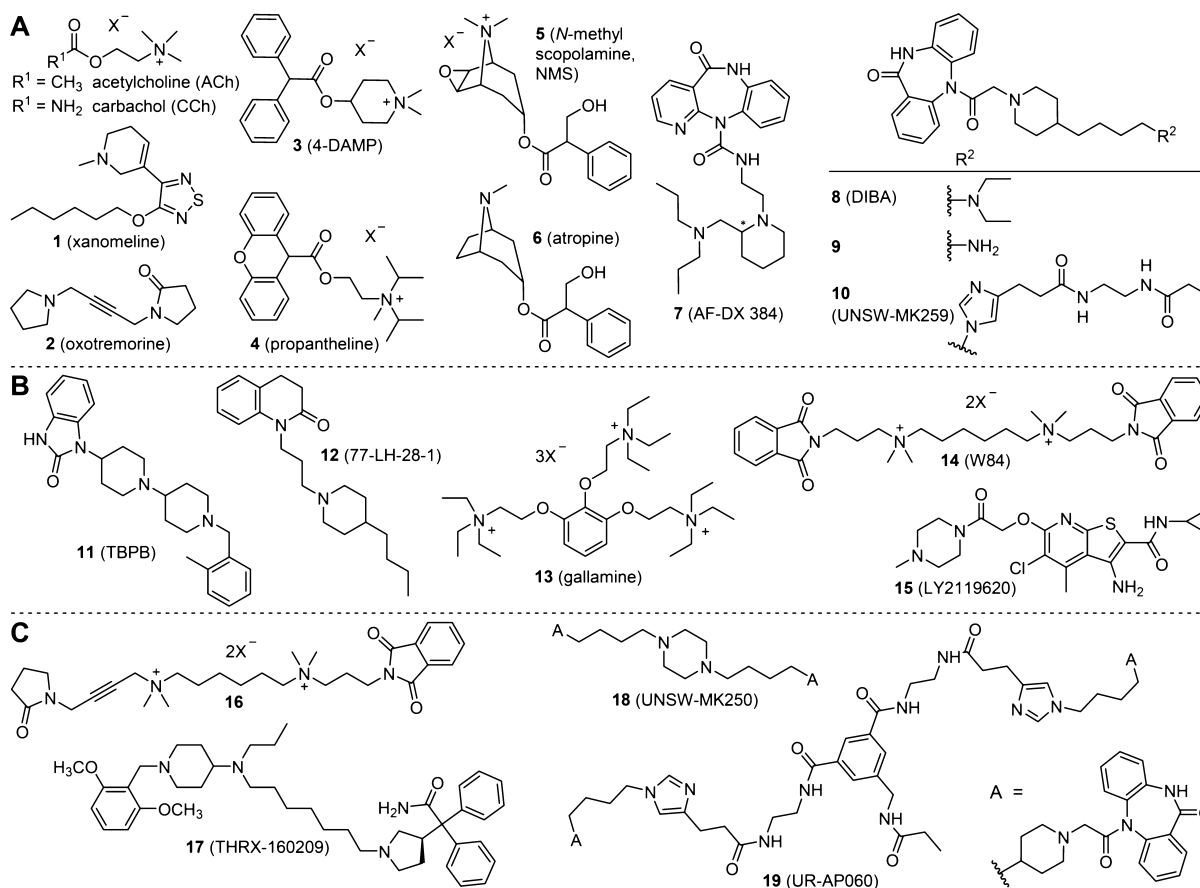


Figure 1. (A) Structures of the described MR agonists (ACh, CCh, 1, and 2) and antagonists (3–10). The M_2R binding poses of compounds 7 and 10 were reported to overlap in part with the binding pose of allosteric M_2R modulator 14.^{21,23} (B) Structures of the selected allosteric MR ligands (compounds 11–15). (C) Structures of heterodimeric ligands 16 and 17 as well as homodimeric MR ligands 18 and 19, the latter suggested to exhibit a dualsteric binding mode at the M_2R .²³

was suggested to bind to the M_2 receptor in a multivalent manner.⁴⁴

Pyridobenzodiazepinone derivative 7 and the structurally closely related dibenzodiazepinone derivative 8 (Figure 1A) represent tricyclic M_2R -preferring MR antagonists.^{45,46} Tränkle et al. suggested a dualsteric binding mode of 7 at the M_2 receptor,²¹ and a hybrid ligand formed of 7 and allosteric modulator 14 was reported to show a pronounced positive cooperativity with 5, pointing at a new way for the development of allosteric enhancers.^{47,48}

This study was aimed at the design, synthesis, and pharmacological evaluation of heterodimeric MR ligands derived from 8, comprising five combinations of 8 with reported orthosteric or allosteric MR ligands: “8–xanomeline (1),” “8–TBPB (11),” “8–77-LH-28-1 (12),” “8–4-DAMP (3),” and “8–proprantheline (4).” Xanomeline (1) (cf. Figure 1A) is a M_1 and M_4 receptor preferring MR agonist.⁴⁹ Compound 11 (cf. Figure 1B) was reported to selectively activate M_1 receptors through an allosteric mechanism, as shown by mutagenesis and molecular pharmacology studies;^{50–52} in other reports, 11 was described as a bitopic M_1R ligand.⁵³ Likewise, compound 12 (cf. Figure 1B) was suggested to be a bitopic M_1R ligand.⁵⁴ MR antagonists 3 and 4 (cf. Figure 1A) are nonselective orthosteric MR antagonists with high affinities [K_i (3, M_1R – M_2R): 0.52–3.80 nM and K_i (4, M_1R – M_4R): 0.057–0.33 nM].^{45,55} In addition to the heterodimeric ligands, one monomeric and four homodimeric

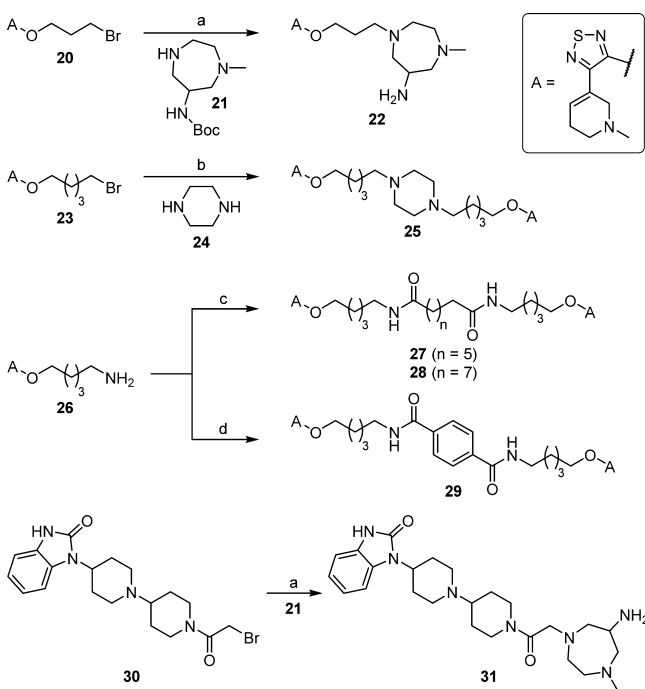
ligands derived from xanomeline, one monomeric and two homodimeric ligands derived from 8, and a monomeric ligand derived from 11 were prepared as reference compounds. Furthermore, two radiolabeled heterodimeric ligands (types “8–11” and “8–1”) were prepared and characterized by saturation binding [including experiments in the presence of allosteric modulators (Schild-like analysis)], kinetic investigations, and competition-binding studies.

2. RESULTS AND DISCUSSION

2.1. Chemistry. Monomeric reference compound 22 and homodimeric xanomeline-derived ligand 25 were prepared by N-alkylation of homopiperazine derivative 21 using bromide 20 [followed by removal of the *tert*-butoxycarbonyl (Boc) group] and by alkylation of piperazine (24) using bromide 23, respectively (Scheme 1). Treatment of amine 26 with octanedioyl dichloride or decanedioyl dichloride in the presence of triethylamine yielded homodimeric xanomeline-type compounds 27 and 28, respectively. Likewise, amidation of terephthalic acid with amine 26, using 1-ethyl-3-(3-dimethylaminopropyl)carbodiimide (EDC)/1-hydroxybenzotriazole hydrate (HOBt) as coupling reagent, afforded homodimeric ligand 29 containing a rigid central linker moiety. N-alkylation of 21 using bromide 30, followed by removal of the Boc group, afforded TBPB derivative 31 (Scheme 1).

The “8–11” type heterodimeric ligand 34 was prepared by N-alkylation of compound 32 using bromide 33; N-alkylation

Scheme 1. Synthesis of Xanomeline Derivatives 22, 25, and 27–29 as well as TBPB Derivative 31^a



^aReagents and conditions: (a) (1) K_2CO_3 , MeCN, microwave 110 °C, 30 min; (2) trifluoroacetic acid (TFA)/ CH_2Cl_2 1:4 v/v, room temperature (rt), 8 h, 66% (22), 20% (31); (b) K_2CO_3 , MeCN, microwave 110 °C, 30 min, 22%; (c) octanedioyl dichloride or decanedioyl dichloride, triethylamine, tetrahydrofuran (THF), 0 °C/rt, overnight, 39% (27), 65% (28); (d) terephthalic acid, EDC, HOBT, dimethylformamide (DMF), rt, overnight, 26%.

of **21** using **33**, followed by removal of the Boc group yielded monomeric reference compound **35** (Scheme 2). Likewise, N-alkylation of piperazine derivatives **36** and **37**, using bromide **33**, gave the “8–4” type heterodimeric ligands **38** and **39**. The “8–1” type heterodimeric ligand **43** was prepared through N-alkylation of compound **40** by applying a mixture of bromides **20** and **33**, followed by Boc-deprotection (Scheme 2). Homodimeric ligand **41**,²³ obtained as a “byproduct” (after Boc-deprotection), was isolated as well. Compound **41** was recently used as an amine precursor for the preparation of a tritium-labeled homodimeric MR ligand.²³ Amine **43** was propionylated to give congener **44**. The “8–1” type ligand **46** was obtained by N-alkylation of **45** by bromide **33** (Scheme 2). The “8–3” type heterodimeric ligand **48** and the “8–12” type ligand **50** were synthesized by alkylation of compound **47** using bromide **33** and by alkylation of amine **9**²² (cf. Figure 1A) using bromide **49**, respectively (Scheme 2). Treatment of **40** with a mixture of bromides **30** and **33**, followed by Boc-deprotection, gave the “8–11” type heterodimeric ligand **51**, which contains a rigid homopiperazine moiety in between the pharmacophores. As in the case of the synthesis of **43**, homodimeric “byproduct” **41** was isolated. Propionylation of **51** gave congener **52** (Scheme 2). Homodimeric ligand **54** was obtained by treating an excess of compound **47** with bromide **53** (Scheme 2). Regarding the syntheses of **43** and **51**, it should be mentioned that the respective non-DIBA type homodimeric ligands, resulting from a double alkylation of **40** with bromides **20** or **30**, were formed as well, but were not isolated because of

interference with other impurities [preparative high-performance liquid chromatography (HPLC)].

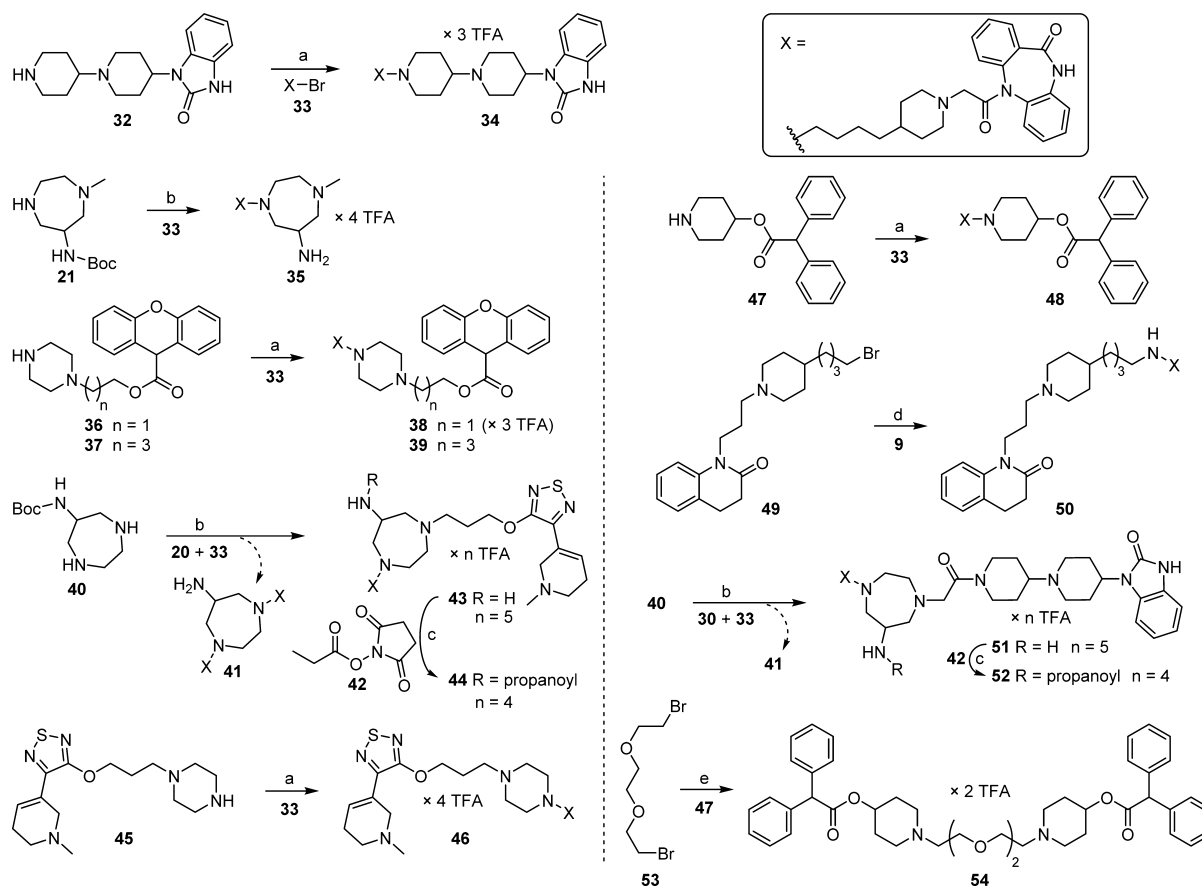
Amidation of isophthalic acid derivative **57** by applying a mixture of amines **55** and **56**, followed by Boc-deprotection, afforded heterodimeric ligand **60** and homodimeric ligand **58** (Scheme 3). Propionylation of **58** and **60** gave congeners **59** and **61**, respectively. By analogy, heterodimeric ligands **63**, **66**, **69**, and **72** were obtained by amidation of **57** using the amine mixtures **55/62**, **55/65**, **55/68**, and **55/71**, respectively, and subsequent Boc-deprotection (Scheme 3). Propionylation of **63**, **66**, and **69** at the central linker moiety afforded propionamide congeners **64**, **67**, and **70**. It should be noted that the respective non-DIBA type homodimeric ligands, generated by double amidation of **57** with amines **56**, **62**, **65**, **68**, or **71**, were formed but were not isolated (cf. Scheme 3).

2.2. Competition Binding at the Human MR Subtypes M_{1-5} with [³H]N-Methylscopolamine ([³H]5) as the Radioligand. **2.2.1. M_2R Affinity.** M_2R receptor-binding affinities of monomeric reference ligands **22**, **31**, and **35**, homodimeric ligands **54** (type “3–3”), **58**, **59** (type “8–8”), and **25**, **27–29** (type “1–1”), as well as heterodimeric ligands **43**, **44**, **46**, **60**, and **61** (type “8–1”), **34**, **51**, **52**, **63**, and **64** (type “8–11”), **50** and **72** (type “8–12”), **38**, **39**, **69**, and **70** (type “8–4”), and **48**, **66**, and **67** (type “8–3”) were determined at live CHO-h M_2R cells in equilibrium-binding experiments using the MR antagonist [³H]5 as the orthosterically binding radioligand. The results are summarized in Table 1.

All compounds containing a dibenzodiazepinone moiety showed high M_2R affinity ($pK_i > 8.3$). Whereas homodimeric derivatives (**25**, **27–29**) of MR agonist **1** exhibited an increased M_2R affinity ($pK_i > 7.7$) compared to the parent compound (pK_i of **1**: 6.55, see Table 3); the opposite was found in the case of MR antagonist **3** [$pK_i = 7.09 \pm 0.04$, mean \pm standard error of the mean (SEM) from two independent experiments] and a homodimeric derivative of **3** (compound **54**, $pK_i = 6.05$, Table 1). The “8–1” type heterodimeric ligand **46** displayed the highest M_2R affinity ($pK_i = 10.14$, Table 1). Steep curve slopes (≤ -1.79) were observed for **43**, **51**, **60**, **61**, **64**, **67**, and **70**, indicating a complex mechanism of binding (e.g., the involvement of more than one binding site).

2.2.2. MR Receptor Subtype Selectivity. Selected dibenzodiazepinone-type heterodimeric ligands (**34**, **38**, **39**, **44**, **46**, **48**, **50**, **52**, **61**, **64**, **67**, **70**, and **72**) and monomeric dibenzodiazepinone derivative **35**, containing an amino-functionalized homopiperazine moiety, were also investigated by equilibrium competition binding at the MR subtypes M_1 , M_3 , M_4 , and M_5 with [³H]5 as the radioligand (Table 1). For all compounds, there was a preference for the M_2R . Except for **38**, the M_1R and M_4R affinities were higher than the M_3R and M_5R affinities, that is, the selectivity profile was $M_2 > M_1 \approx M_4 > M_3/M_5$ (**34**, **39**, **44**, **46**, **48**, **50**, **52**, **61**, **64**, **67**, **70**, and **72**) and $M_2 > M_1 \approx M_5 > M_3 > M_4$ in the case of **38** (Table 1). Compound **46**, showing the highest M_2R affinity among the studied MR ligands, exhibited a more pronounced M_2R selectivity than the pyridobenzodiazepinone-type ligand **7** (cf. Figure 1A),⁴⁵ the MR antagonist triptamine⁵⁶ containing three pyridobenzodiazepinone moieties, as well as the recently reported dibenzodiazepinone derivatives **10** and **19** (cf. Figure 1C).²³ Displacement of [³H]5 by **46** as well as by heterodimeric ligands **44** and **64**, which were prepared as tritiated ligands (see below), from M_xR s (determined at CHO-h M_xR cells, $x = 1–5$) is illustrated in Figure 2.

Scheme 2. Synthesis of DIBA (8)-Derived Heterodimeric Ligands **34**, **38**, **39**, **43**, **44**, **46**, **48**, and **50–52**, Monomeric Dibenzodiazepinone Derivative **35**, and 4-DAMP (3)-Derived Homodimeric Ligand **54**^a



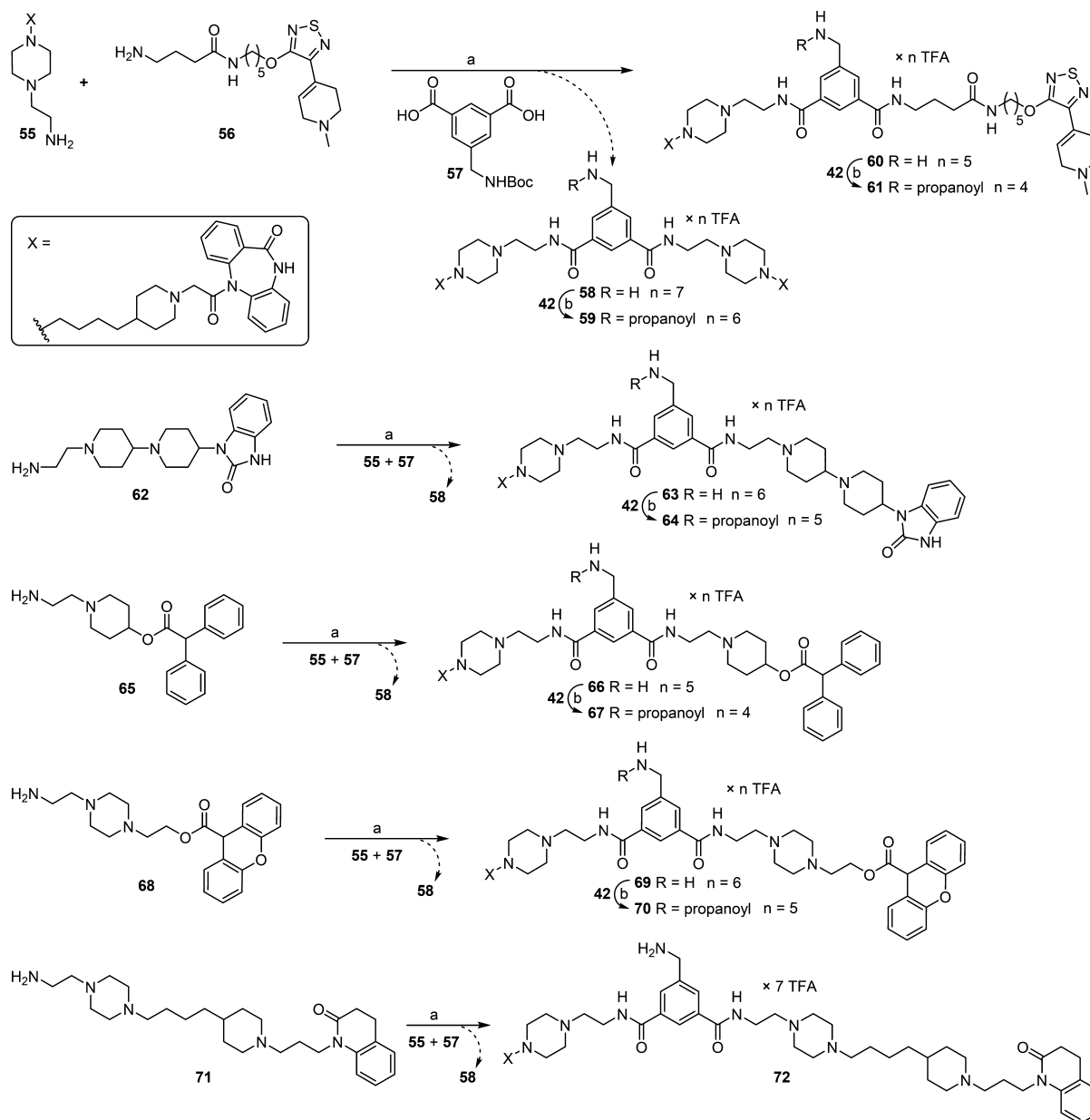
^aReagents and conditions: (a) K_2CO_3 , MeCN, reflux, 3–6 h, 57% (**34**), 51% (**38**), 38% (**39**), 41% (**46**), 27% (**48**); (b) (1) K_2CO_3 , MeCN, reflux (3 h or overnight) or microwave 110 °C (30 min); (2) TFA/ CH_2Cl_2 / H_2O 10:10:1 v/v/v, rt, 2 h, 12% (**35**), 17% (**43**), 12% (**51**); (c) diisopropylethylamine (DIPEA), DMF, rt, 2 h, 95% (**44**), 96% (**52**); (d) NaI, K_2CO_3 , MeCN, reflux, 3 h, 52%; (e) K_2CO_3 , MeCN, microwave 110 °C, 45 min, 23%.

2.3. Effect on IP1 Accumulation. As previously reported for homodimeric dibenzodiazepinone derivative **19**,²³ the homodimeric xanomeline-type ligand **25** and the heterodimeric dibenzodiazepinone-type ligands **44**, **46**, and **64** were investigated with respect to M_2R agonism and antagonism in an IP accumulation assay (Figure 3). Like **19**, compounds **44**, **46**, and **64** did not induce an IP1 accumulation when investigated in the agonist mode (Figure 3A), but completely suppressed the effect of CCh when studied in the antagonist mode (Figure 3B), revealing that the combination of the agonist xanomeline (**1**) with a dibenzodiazepinone-type antagonist in one molecule (e.g., **44**) resulted in a loss of agonistic activity. Interestingly, homodimeric ligand **25**, which is derived from MR agonist **1**, proved to be a M_2R antagonist in contrast to parent compound **1** (Figure 3). The pK_b values of **44**, **46**, and **64** (cf. Figure 3B) were lower compared to the respective pK_i values (cf. Table 1), as previously observed for homodimeric ligand **19**.²³ Possible reasons for this discrepancy are discussed elsewhere.²³

2.4. Synthesis of the Radiolabeled Ligands [³H]44** and [³H]**64**.** Aiming at a radiolabeled derivative of heterodimeric ligand **46**, which exhibited the highest M_2R affinity and selectivity (cf. Table 1), compound **44**, containing a propionamido-substituted homopiperazine moiety instead of the piperazine ring in **46** (cf. Scheme 2), was prepared as a

tritiated derivative from amine precursor **43** and commercially available [³H]**42** (Figure 4A). Additionally, the tritiated derivative of heterodimeric ligand **64** was prepared from **63** and [³H]**42** (Figure 4A). The chemical stabilities of the “cold” analogues **44** and **64** were investigated under assaylike conditions [phosphate-buffered saline (PBS) pH 7.4] for over 48 h. **44** and **64** proved to be stable under these conditions (cf. SI Figure 1, Supporting Information). [³H]**44** and [³H]**64** were obtained in high radiochemical purities (98% and 99%, respectively; Figure 4B,D) and showed a high ([³H]**44**) and excellent ([³H]**64**) stability when stored in ethanol at −20 °C (cf. Figure 4C,E).

2.5. Characterization of [³H]44** and [³H]**64**.** Saturation-binding experiments with [³H]**44** and [³H]**64** at intact CHO-h M_2R cells or CHO-h M_2R cell homogenates yielded monophasic saturation isotherms (Figure 5). As previously reported for [³H]**19**,²³ the extent of unspecific binding strongly depended on the assay conditions: in the case of experiments performed at intact adherent cells (white/transparent 96-well plates), unspecific binding was considerably higher compared to experiments performed at cell homogenates, which preclude the unspecific binding of the radioligand to the microplate (Figure 5).²³ The apparent K_d values amounted to 1.0 and 0.081 nM (cell homogenates, Table 2). As orthosteric antagonist **6** (used to determine unspecific binding) completely

Scheme 3. Synthesis of Dibenzodiazepinone-Type Homo- or Heterodimeric Ligands 58–61, 63, 64, 66, 67, 69, 70, and 72^a

^aReagents and conditions: (a) (1) 2-(1H-benzotriazole-1-yl)-1,1,3,3-tetramethylammonium, HOBT, DIPEA, DMF, 60 °C, 3 h; (2) TFA/CH₂Cl₂/H₂O 10:10:1 v/v/v, rt, 2 h, 8% (58), 16% (60), 10% (63), 28% (66), 15% (69), 4% (72); (b) DIPEA, DMF, rt, 2 h, 79% (59), 89% (61), 88% (64), 83% (67), 86% (70).

prevented hyperbolic (monophasic) binding of the radioligands to the M₂R, these experiments proved that [³H]44 and [³H]64 bind to the orthosteric binding site of the M₂R, as previously reported for [³H]19.²³

The association of [³H]44 and [³H]64 with the human M₂R was monophasic and yielded similar *k*_{on} values (Figure 6A,C, Table 2). Whereas the “8–1” type heterodimeric ligand [³H]44 dissociated completely from the M₂R (*t*_{1/2} = 47 min, cf. Figure 6B, Table 2), the dissociation of the “8–11” type dimeric ligand [³H]64 was incomplete, reaching a plateau at approximately 47% of initially M₂R-bound [³H]64 (*t*_{1/2} = 35 min, cf. Figure 6D, Table 2). An incomplete ligand dissociation, which might be attributed to conformational adjustments of the receptor upon ligand binding⁵⁷ or an enhanced rebinding capability of the dimeric ligand,⁵⁸ was also reported for the homodimeric

dibenzodiazepinone-type ligand [³H]19.²³ The kinetically derived dissociation constants of both [³H]44 and [³H]64 [*K*_d(kin): 0.33 and 0.057 nM, respectively] were in good accordance with the *K*_d values obtained from the saturation-binding experiments (Table 2).

2.6. Competition Binding at the M₂R Using [³H]44 and [³H]64 as Radioligands. Heterodimeric radioligands [³H]44 and [³H]64 were applied to equilibrium competition-binding experiments at CHO-hM₂R cell homogenates involving various reported orthosteric, dualsteric, and allosteric MR ligands. Orthosteric MR antagonist 6, dualsteric ligand 10, and allosteric modulator 14 (cf. Figure 1) were capable of totally displacing [³H]44 from the M₂R (SI Figure 2A, Supporting Information), indicating either a competitive mechanism or a strongly negative cooperativity between dimeric ligand [³H]44 and 6,

Table 1. MR Affinities (pK_i Values) of Monomeric Reference Compounds 22, 31, and 35, Homodimeric Ligands 25, 27–29, 54, 58, and 59, as well as Heterodimeric Ligands 34, 38, 39, 43, 44, 46, 48, 50–52, 60, 61, 63, 64, 66, 67, 69, 70, and 72 Obtained from Equilibrium Competition-Binding Studies with [³H]5 at Live CHO-hM_xR Cells (x = 1–5)

Cmpd.	M ₁ R		M ₂ R		M ₃ R		M ₄ R		M ₅ R	
	pK _i	slope ^a	pK _i	slope ^a	pK _i	slope ^a	pK _i	slope ^a	pK _i	slope ^a
22	n.d.	n.d.	4.90 ± 0.16	-1.01 ± 0.10	n.d.	n.d.	n.d.	n.d.	n.d.	n.d.
25	7.36 ± 0.10	-1.04 ± 0.07	7.75 ± 0.18	-0.92 ± 0.18	7.30 ± 0.02	-0.95 ± 0.04	n.d.	n.d.	n.d.	n.d.
27	8.30 ± 0.08	-0.89 ± 0.10	8.46 ± 0.17	-0.94 ± 0.08	8.14 ± 0.04	-1.14 ± 0.03	n.d.	n.d.	n.d.	n.d.
28	8.41 ± 0.05	-1.30 ± 0.05	8.67 ± 0.11	-0.84 ± 0.07	n.d.	n.d.	n.d.	n.d.	n.d.	n.d.
29	7.72 ± 0.13	-1.15 ± 0.18	8.38 ± 0.13	-0.83 ± 0.06	n.d.	n.d.	n.d.	n.d.	n.d.	n.d.
31	n.d.	n.d.	5.88 ± 0.29	-0.87 ± 0.05	n.d.	n.d.	n.d.	n.d.	n.d.	n.d.
34	8.57 ± 0.05	-1.13 ± 0.05	9.12 ± 0.05	-1.43 ± 0.20	7.01 ± 0.11	-1.12 ± 0.07	7.95 ± 0.50	-1.18 ± 0.06	7.09 ± 0.07	-1.09 ± 0.20
35	7.26 ± 0.10	0.92 ± 0.08	8.67 ± 0.03	-0.87 ± 0.09	6.25 ± 0.06	-0.93 ± 0.20	8.00 ± 0.01	-0.77 ± 0.02 ^b	6.86 ± 0.17	-1.09 ± 0.15
38	8.47 ± 0.08	-1.03 ± 0.12	8.82 ± 0.14	-1.08 ± 0.22	8.12 ± 0.05	-1.36 ± 0.09	7.99 ± 0.28	-0.98 ± 0.12	8.47 ± 0.06	-1.17 ± 0.10
39	7.62 ± 0.19	-1.40 ± 0.30	8.37 ± 0.28	-1.51 ± 0.26	7.01 ± 0.10	-0.85 ± 0.04	7.52 ± 0.35	-1.25 ± 0.10	7.03 ± 0.03	-1.09 ± 0.18
43	8.35 ± 0.07	-1.47 ± 0.17	9.30 ± 0.05	-2.19 ± 0.06 ^b	7.21 ± 0.04	-1.34 ± 0.16	n.d.	n.d.	n.d.	n.d.
44	8.39 ± 0.03	-1.05 ± 0.05	9.34 ± 0.03	-1.14 ± 0.07	6.84 ± 0.03	-0.93 ± 0.04	8.24 ± 0.08	-0.94 ± 0.06	7.00 ± 0.09	-1.21 ± 0.19
46	8.84 ± 0.11	-1.45 ± 0.02 ^b	10.14 ± 0.11	-0.96 ± 0.05	7.88 ± 0.06	-1.17 ± 0.08	8.59 ± 0.05	-1.17 ± 0.04	7.47 ± 0.03	-1.07 ± 0.22
48	7.68 ± 0.12	-1.03 ± 0.22	8.66 ± 0.03	-1.24 ± 0.22	7.46 ± 0.12	-1.35 ± 0.06 ^b	8.07 ± 0.19	-1.17 ± 0.11	7.27 ± 0.05	-1.11 ± 0.10
50	8.40 ± 0.08	-1.00 ± 0.05	9.24 ± 0.11	-1.38 ± 0.22	6.86 ± 0.04	-1.05 ± 0.09	8.48 ± 0.03	-1.4 ± 0.06	7.03 ± 0.07	-1.01 ± 0.25
51	8.37 ± 0.03	-1.47 ± 0.05 ^b	9.16 ± 0.07	-1.86 ± 0.05 ^b	7.23 ± 0.06	-1.05 ± 0.10	n.d.	n.d.	n.d.	n.d.
52	7.78 ± 0.08	-1.82 ± 0.19 ^b	9.11 ± 0.10	-1.12 ± 0.15	6.23 ± 0.10	-1.01 ± 0.03	8.10 ± 0.11	-0.85 ± 0.07	6.88 ± 0.10	-1.31 ± 0.10
54	6.59 ± 0.07	-1.14 ± 0.12	6.05 ± 0.06	-1.33 ± 0.18	5.64 ± 0.09	-1.05 ± 0.34	5.63 ± 0.04	-1.00 ± 0.06	5.87 ± 0.25	-1.35 ± 0.20
58	8.69 ± 0.09	-2.06 ± 0.19 ^b	9.83 ± 0.07	-1.53 ± 0.15	7.78 ± 0.05	-1.27 ± 0.10	n.d.	n.d.	n.d.	n.d.
59	8.53 ± 0.08	-1.75 ± 0.34	9.24 ± 0.06	-1.31 ± 0.09	7.89 ± 0.07	-1.22 ± 0.09	7.89 ± 0.07	-1.22 ± 0.09	n.d.	n.d.
60	8.80 ± 0.10	-1.32 ± 0.31	9.65 ± 0.15	-1.79 ± 0.09 ^b	7.76 ± 0.14	-1.28 ± 0.04 ^b	n.d.	n.d.	n.d.	n.d.
61	8.88 ± 0.08	-1.61 ± 0.03 ^b	9.47 ± 0.07	-2.37 ± 0.15 ^b	7.87 ± 0.02	-0.99 ± 0.04	8.87 ± 0.08	-1.14 ± 0.11	8.37 ± 0.24	-1.02 ± 0.11
63	8.79 ± 0.09	-1.19 ± 0.07	9.71 ± 0.08	-1.37 ± 0.14	7.77 ± 0.03	-1.22 ± 0.05	n.d.	n.d.	n.d.	n.d.
64	8.56 ± 0.11	-1.59 ± 0.15	9.44 ± 0.06	-1.84 ± 0.17 ^b	7.55 ± 0.04	-1.40 ± 0.10	8.57 ± 0.02	-1.01 ± 0.04	6.96 ± 0.04	-1.26 ± 0.14
66	8.28 ± 0.05	-1.32 ± 0.19	9.16 ± 0.20	-1.64 ± 0.23	7.20 ± 0.19	-1.33 ± 0.08	n.d.	n.d.	n.d.	n.d.
67	8.38 ± 0.06	-1.54 ± 0.14	8.94 ± 0.07	-2.14 ± 0.16 ^b	7.52 ± 0.04	-1.25 ± 0.09	8.50 ± 0.08	-1.52 ± 0.26	7.62 ± 0.06	-1.51 ± 0.12
69	8.42 ± 0.19	-1.74 ± 0.19	9.17 ± 0.18	-1.52 ± 0.31	7.26 ± 0.22	-1.23 ± 0.12	n.d.	n.d.	n.d.	n.d.
70	8.51 ± 0.13	-1.10 ± 0.07	8.96 ± 0.08	-2.14 ± 0.18 ^b	7.72 ± 0.06	-1.21 ± 0.13	8.29 ± 0.02	-1.41 ± 0.05 ^b	7.37 ± 0.08	-1.01 ± 0.12
72	8.52 ± 0.09	-1.66 ± 0.20	9.63 ± 0.03	-1.31 ± 0.13	7.88 ± 0.03	-1.42 ± 0.09 ^b	8.39 ± 0.09	-1.50 ± 0.17	7.69 ± 0.33	-0.85 ± 0.07

^aCurve slope of the four-parameter logistic fit. Presented are mean values ± SEM from three to five independent experiments (each performed in triplicate). ^bK_d values reported previously²²/applied concentrations of [³H]5; M₁: 0.12/0.2 nM; M₂: 0.090/0.2 nM; M₃: 0.0895/0.2 nM; M₄: 0.040/0.1 nM; and M₅: 0.24/0.3 nM. ^cSlope different from unity (P < 0.05).

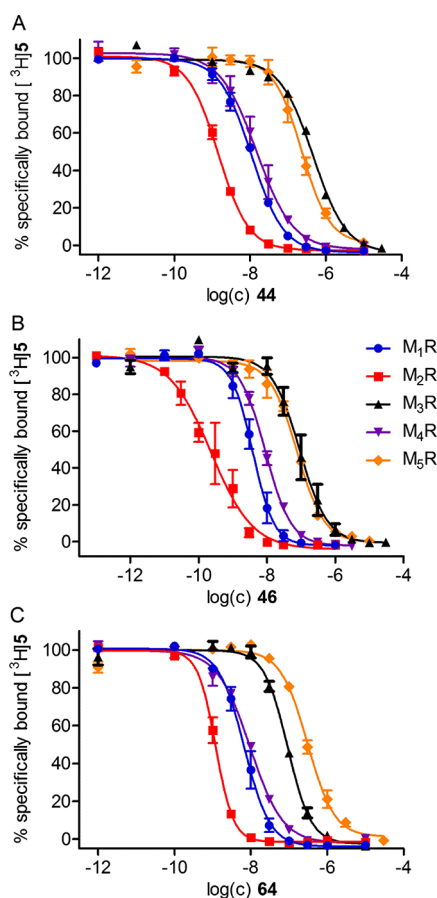


Figure 2. Displacement of [^3H]5 [$c = 0.2 \text{ nM}$ (M_1 , M_2 , M_3), 0.1 nM (M_4), or 0.3 nM (M_5)] by heterodimeric ligands **44** (A), **46** (B), and **64** (C) from M_x R s determined at intact CHO-h M_x R cells ($x = 1-5$). Data represent mean values \pm SEM from at least three independent experiments (performed in triplicate).

10, or **14**. Likewise, orthosteric ligands **1** and **6**, dualsteric ligands **7** and **10**, as well as allosteric modulators **13-15** (cf. Figure 1) completely displaced [^3H]64 from the M_2 R-specific binding sites. (SI Figure 2B, Supporting Information). For most of the investigated MR ligands, the respective pK_i values were in good agreement with the binding data obtained from competition binding with [^3H]5 (Table 3). However, the pK_i values of compounds **1**, **6**, **7**, and **10**, determined in the presence of [^3H]64, were consistently lower (up to 1 log unit in the case of **7**) than pK_i values from the competition-binding experiments with [^3H]5. This is in agreement with the (in part) irreversible M_2 R binding of [^3H]64 (cf. Figure 6D), which compromises its use as a molecular tool for the determination of binding constants of nonlabeled ligands, as was also reported for homodimeric MR ligand [^3H]19.²³

2.7. Schild-like Analysis with [^3H]64 and Allosteric M_2 R Modulator 14. To further explore the binding mode of heterodimeric ligand **64** at the M_2 R, saturation-binding experiments were performed with [^3H]64 in the presence of increasing concentrations of allosteric M_2 R ligand **14** (Figure 7), as recently reported for homodimeric radioligand [^3H]19.²³ As in the case of [^3H]19,²³ this Schild-like analysis resulted in rightward-shifted saturation isotherms of [^3H]64 (Figure 7A) and a linear Schild plot with a slope not different from unity (Figure 7B), which is consistent with a competitive mechanism between [^3H]64 and allosteric M_2 R ligand **14**. With regard to

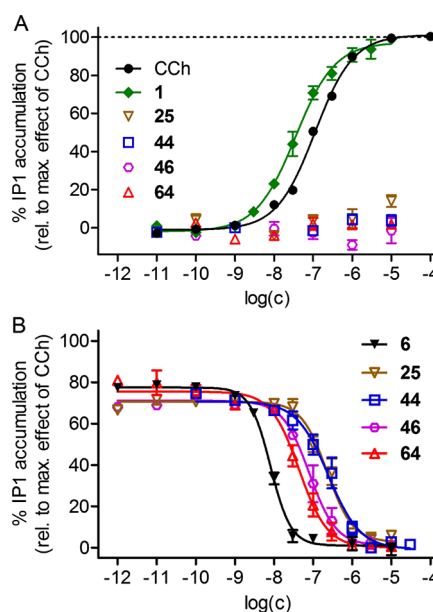


Figure 3. M_2 R agonism and antagonism of **25**, **44**, **46**, and **64** investigated in an IP1 accumulation assay using HEK-h M_2 -G α_{q15} -HA cells. (A) Concentration-dependent effect of CCh, **1**, **25**, **44**, **46**, and **64** on the accumulation of IP1. **25**, **44**, **46**, and **64** elicited no response. pEC_{50} of CCh and **1**: 6.96 and 7.45, respectively. Data represent mean values \pm SEM from at least seven (CCh and **1**) or at least two (**25**, **44**, **46**, and **64**) independent experiments (each performed in triplicate). (B) Concentration-dependent inhibition of the IP1 accumulation induced by CCh ($0.3 \mu\text{M}$) by **6**, **25**, **44**, **46**, and **64**. Corresponding pK_b values: **6**: 8.63,²³ **25**: 7.21, **44**: 7.18, **46**: 7.67, and **64**: 7.93. Data represent mean values \pm SEM from at least five independent experiments (each performed in duplicate).

the fact that [^3H]64 binds to the orthosteric binding site of the M_2 R (see above), these results strongly support a dualsteric binding mode of **64** at the human M_2 R. The “ pA_2 ” value of 7.16, obtained for **14** from the Schild regression (Figure 7B), was in accordance with the reported M_2 R binding data of **14** (pK_x 7.50⁵⁹).

3. CONCLUSIONS

Linking orthosteric (**1**, **3**, and **4**) and allosteric (**11** and **12**) MR ligands with a M_2 R preferring dibenzodiazepinone-type MR antagonist (**8**) yielded a series of heterodimeric ligands (**34**, **38**, **39**, **43**, **44**, **46**, **48**, **50-52**, **60**, **61**, **63**, **64**, **66**, **67**, **69**, **70**, and **72**). The “8-1” type dimeric ligand **46** (UR-SK75), containing a piperazine moiety in the linker, exhibited a higher M_2 R affinity (pK_i 10.14) and selectivity [expressed as the ratio of K_i values ($M_1/M_2/M_3/M_4/M_5$): 23:1:180:29:430] compared to monomeric (such as **8**⁴⁶ and **10**^{22,23}) and homodimeric (e.g., **18**²² and **19**²³) dibenzodiazepinone-type ligands. High M_2 R affinity of all dibenzodiazepinone-type heterodimeric ligands ($pK_i > 8.3$, Table 1), as also reported for monomeric dibenzodiazepinone-type ligands,²² suggested a minor influence of the second pharmacophore on M_2 R binding, indicating that the high M_2 R affinity of these compounds is mediated by the “dibenzodiazepinone” pharmacophore, which binds most likely to the orthosteric binding site of the M_2 R. This is supported by the proposed binding mode of **10** and **19** at the M_2 R,²³ by saturation-binding studies using the radioligands [^3H]44 ([^3H]UR-SK71) and [^3H]64 ([^3H]UR-SK59), and by the fact that compounds containing M_1 R/ M_4 R selective agonist **1**⁴⁹

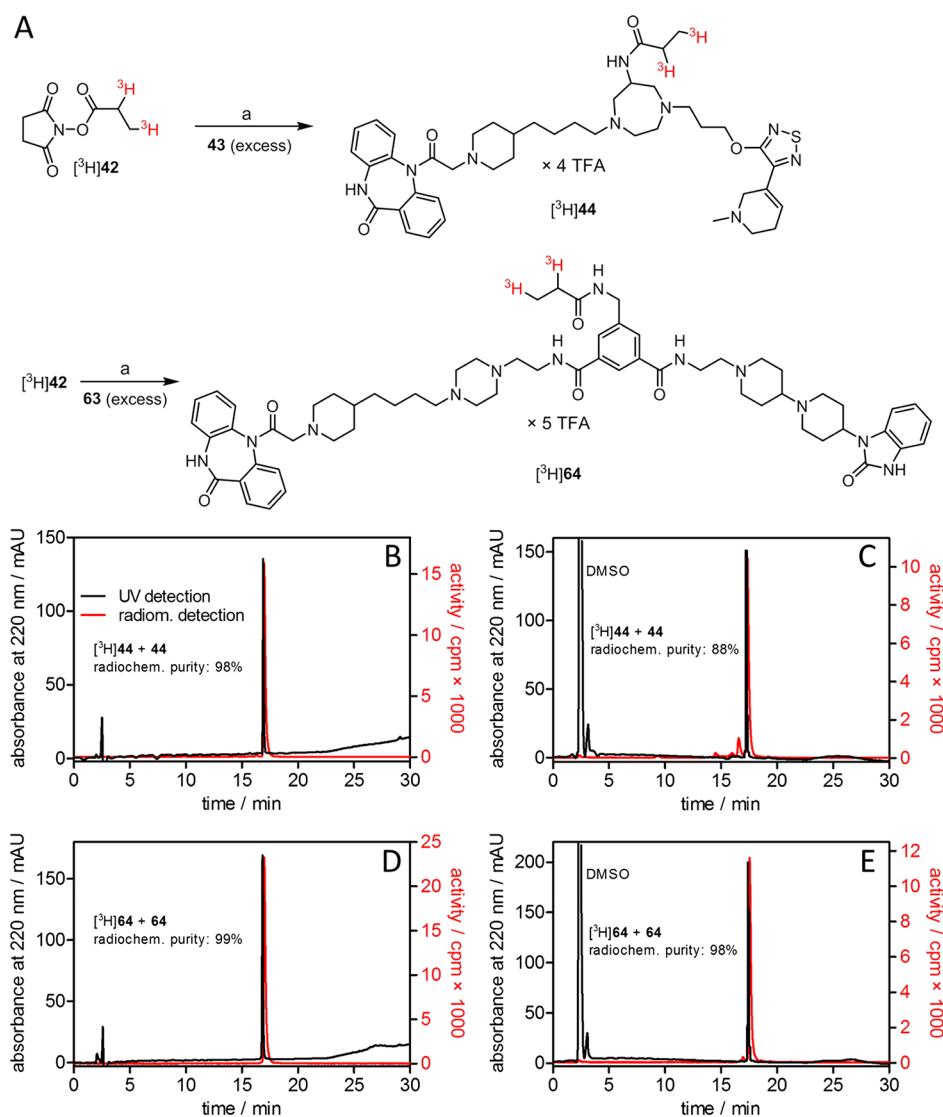


Figure 4. Preparation, purity, and identity control of the radiolabeled dibenzodiazepinone derivatives $[^3\text{H}]44$ and $[^3\text{H}]64$. (A) Synthesis of $[^3\text{H}]44$ and $[^3\text{H}]64$ by $[^3\text{H}]$ propionylation of amine precursors **43** and **63**, respectively, using succinimidyl $[^3\text{H}]$ propionate ($[^3\text{H}]42$). Reagents and conditions: (a) DIPEA, DMF, rt, 1.5 h, radiochemical yields: 36% ($[^3\text{H}]44$) and 35% ($[^3\text{H}]64$). (B,C) HPLC analysis of $[^3\text{H}]44$ ($0.18 \mu\text{M}$) spiked with “cold” **44** ($3 \mu\text{M}$), analyzed 3 days after synthesis (B) and after 10 months of storage at -20°C in EtOH/ H_2O (1:1) (C). (D,E) HPLC analysis of $[^3\text{H}]64$ ($0.23 \mu\text{M}$) spiked with “cold” **64** ($3 \mu\text{M}$), analyzed 3 days after synthesis (D) and after 10 months of storage at -20°C in EtOH/ H_2O (1:1) (E). HPLC conditions are provided in the Supporting Information.

as a second pharmacophore (**43**, **44**, **46**, **60**, and **61**) proved to be M_2R -preferring ligands. Moreover, the prototypical heterodimeric ligands **44** and **46** were shown to be M_2R antagonists (cf. Figure 3). Concerning the “8–1” type heterodimeric ligands, one can speculate about the contribution of the pharmacophore of **1** to M_2R binding because the homodimeric derivatives of **1** (compounds **25**, **27–29**) exhibited considerably higher M_2R affinities compared to **1**. This work confirms that dibenzodiazepinone-type MR ligands represent a promising class of compounds for the development of highly selective M_2R ligands with a high receptor affinity based on the dualsteric ligand approach.

4. METHODS

4.1. General Experimental Conditions. Reagents and chemicals for synthesis were purchased from Acros Organics (Geel, Belgium), Iris Biotech (Marktredwitz, Germany), Alfa Aesar (Karlsruhe, Germany), Merck (Darmstadt, Germany),

Sigma (Munich, Germany), or TCI Europe (Zwijndrecht, Belgium). Technical grade solvents (acetone, ethyl acetate, light petroleum ($40\text{--}60^\circ\text{C}$), and CH_2Cl_2) were distilled before use. Deuterated solvents for nuclear magnetic resonance (NMR) spectroscopy were from Deutero (Kastellaun, Germany). Acetonitrile for HPLC (gradient grade) was obtained from Merck or Sigma. Anhydrous DMF was purchased from Sigma. CCh (Sigma) and compounds **6** (Sigma), **7** (Abcam, Cambridge, UK), **13** (Sigma), **14** (Sigma), and **15** (Absource Diagnostic, Munich, Germany) were purchased from commercial suppliers. The radiolabeled MR antagonist $[^3\text{H}]5$ (specific activity = 80 Ci/mmol) was purchased from American Radiolabeled Chemicals Inc. (St. Louis, MO) via Hartmann Analytic (Braunschweig, Germany). The syntheses of compounds **40**,²³ **42**,⁶⁰ and **57**²³ are described elsewhere. Compounds **1**,⁶¹ **120**,²³ and **123**⁶² were prepared according to described procedures.

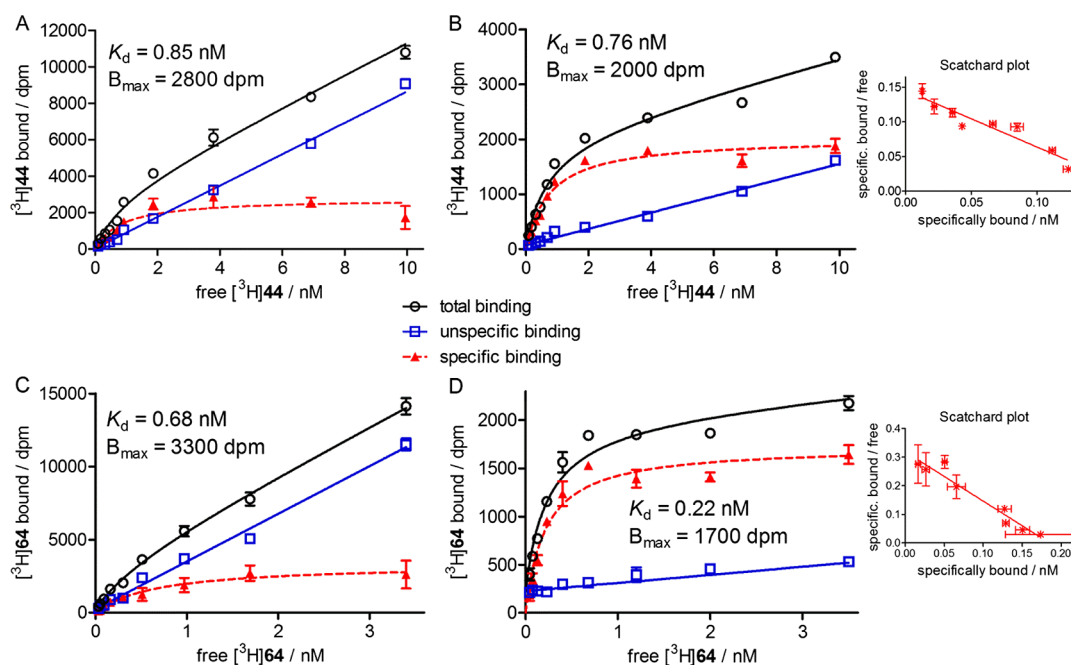


Figure 5. Representative hyperbolic (monophasic) isotherms of specific M_2R binding (red dashed line) of $[^3H]44$ (A,B) and $[^3H]64$ (C,D) obtained from saturation-binding experiments either performed with live adherent CHO-h M_2R cells (A,C) or CHO-h M_2R cell homogenates (B,D). Unspecific binding (blue solid line) was determined in the presence of MR antagonist **6** (500-fold excess). Experiments were performed in triplicate. The error bars of specific binding and error bars in the Scatchard plots represent propagated errors calculated according to the Gaussian law of errors. The error bars of total and unspecific binding represent the SEM.

Table 2. M_2R Binding Characteristics of $[^3H]44$ and $[^3H]64$

radioligand	saturation-binding		binding kinetics	
	K_d [nM] ^a	K_d (kin) [nM] ^b	k_{on} [min ⁻¹ nM ⁻¹] ^c	k_{off} [min ⁻¹] ^d , $t_{1/2}$ [min] ^d
$[^3H]44$	1.0 ± 0.2	0.20 ± 0.03	0.078 ± 0.015	0.015 ± 0.001, 47 ± 3
$[^3H]64$	0.081 ± 0.022	0.072 ± 0.002	0.31 ± 0.01	0.022 ± 0.002, 35 ± 1

^aDissociation constant determined by saturation binding at CHO-h M_2R cell homogenates; mean ± SEM from at least three independent experiments (performed in triplicate). ^bKinetically derived dissociation constant ± propagated error [K_d (kin) = k_{off}/k_{on}]. ^cAssociation rate constant ± propagated error, calculated from k_{obs} (nonlinear regression), k_{off} (nonlinear regression), and the applied radioligand concentration (cf. Radioligand Binding). ^dDissociation rate constant (nonlinear regression, two ($[^3H]44$)- or three ($[^3H]64$)-parameter equation describing a monophasic decline) and half-life; mean ± SEM from three independent experiments (performed in triplicate).

Millipore water was used throughout for the preparation of buffers and HPLC eluents. If moisture-free conditions were required, reactions were performed in dried glassware under an inert atmosphere (argon). Anhydrous THF was obtained by distillation over sodium, and anhydrous CH_2Cl_2 was prepared by distillation over P_2O_5 after predrying over $CaCl_2$. Reactions were monitored by thin-layer chromatography using aluminum plates coated with silica gel (Merck silica gel 60 F₂₅₄, thickness 0.2 mm). Spots were detected by ultraviolet (UV) light (254 or 366 nm) or by staining using 0.3% solution of ninhydrin in *n*-butanol (amines) or iodine. Column chromatography was performed in glass columns on silica gel (Merck silica gel 60, 63–200 μ m). Flash chromatography was performed on an Intelli Flash-310 Flash-Chromatography Workstation (Varian, Darmstadt, Germany). Polypropylene reaction vessels (1.5 or 2 mL) with a screw cap (Süd-Laborbedarf, Gauting, Germany) were used for the synthesis of radioligands ($[^3H]44$ and $[^3H]64$) for small-scale reactions, for the investigation of chemical stabilities (**44** and **64**), and for the preparation and storage of stock solutions. Melting points were measured with a Büchi 530 (Büchi, Essen, Germany) apparatus and are uncorrected. Microwave-assisted reactions were performed with an Initiator

2.0 synthesizer (Biotage, Uppsala, Sweden). NMR spectra were recorded on a Bruker AVANCE 300 (7.05 T), Bruker AVANCE III HD 400 (9.40 T), or a Bruker AVANCE III HD 600 spectrometer equipped with a cryogenic probe (14.1 T) (Bruker, Karlsruhe, Germany). Abbreviations for the multiplicities of the signals are s (singlet), d (doublet), t (triplet), dd (doublet-of-doublet), q (quartet), m (multiplet), and brs (broad-singlet). Infrared (IR) spectra were measured with a Nicolet 380 FT-IR spectrophotometer (Thermo Electron Corporation). Low-resolution mass spectrometry was performed on a Finnigan SSQ 710A instrument [chemical ionization mass spectrometry (CI-MS, Thermo Finnigan, San Jose, CA). High-resolution mass spectrometry (HRMS) analysis was performed on an Agilent 6540 UHD Accurate-Mass Q-TOF LC/MS system (Agilent Technologies, Santa Clara, CA) using an electrospray ionization source. Preparative HPLC was performed on a system from Knauer (Berlin, Germany) consisting of two K-1800 pumps and a K-2001 detector. Except for compound **54**, a Kinetex-XB C18 column, 5 μ m, 250 × 21 mm (Phenomenex, Aschaffenburg, Germany) served as the stationary phase at a flow rate of 15 mL/min. For the purification of **54**, a Nucleodur 100-5 C18 column, 5 μ m,

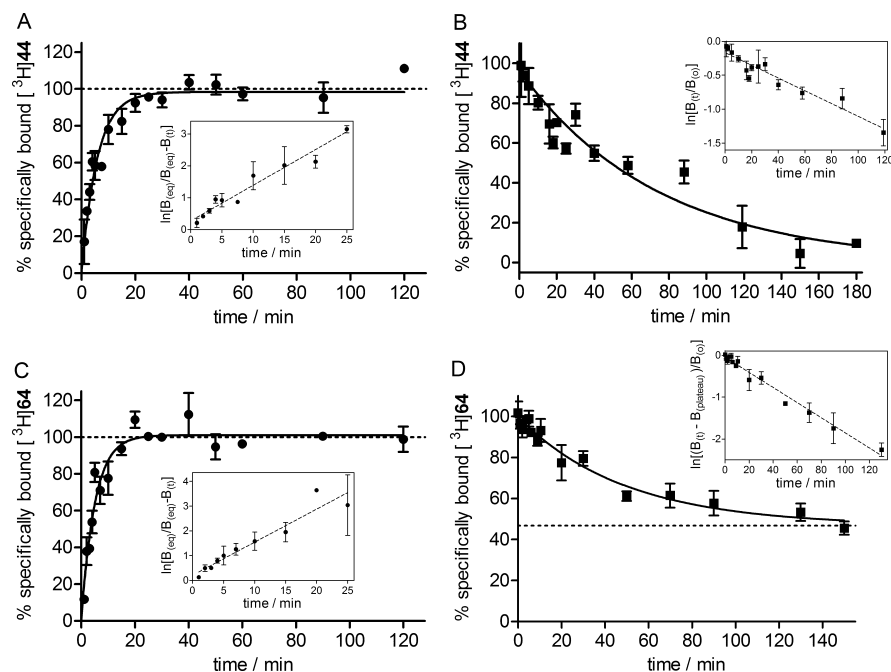


Figure 6. Association and dissociation kinetics of [³H]44 (A,B) and [³H]64 (C,D) determined at CHO-hM₂R cell homogenates at 23 °C. (A) Association of [³H]44 (*c* = 2 nM) with the M₂R. Inset: $\ln[B_{(eq)}/(B_{(eq)} - B_{(t)})]$ vs time. (B) Dissociation of [³H]44 (preincubation: 4 nM, 1 h) from the M₂R determined in the presence of **6** (1000-fold excess), showing complete monophasic exponential decline. Inset: $\ln[B_{(t)}/B_{(0)}]$ vs time. (C) Association of [³H]64 (*c* = 0.6 nM) with the M₂R. Inset: $\ln[B_{(eq)}/(B_{(eq)} - B_{(t)})]$ vs time. (D) Dissociation of [³H]64 (preincubation: 0.6 nM, 1 h) from the M₂R determined in the presence of **6** (1000-fold excess), showing incomplete monophasic exponential decline. Inset: $\ln[(B_{(t)} - B_{(plateau)})/B_{(0)}]$ versus time. For *k*_{on} and *k*_{off} values, see Table 2. Data represent mean ± SEM from three (A,B,D) or two (C) independent experiments (each performed in triplicate).

Table 3. M₂R Binding Data (p*K*_i or p*IC*₅₀ Values) of Various Orthosteric (**1** and **6**), Allosteric (**13–15**), Dualsteric (**7** and **10**) MR Ligands, and **64** Determined with [³H]44, [³H]64, or [³H]5

ligand	[³ H]44 p <i>K</i> _i ^a	[³ H]64 p <i>K</i> _i ^a	[³ H]5 p <i>K</i> _i ^a or p <i>IC</i> ₅₀ ^{*b}
1		5.78 ± 0.05	6.55 ± 0.05*
6	8.52 ± 0.26	8.52 ± 0.14	9.04 ± 0.08*
7		7.71 ± 0.14	8.71 ± 0.05*
10	9.61 ± 0.11	8.35 ± 0.09	9.11 ± 0.05*
13		5.60 ± 0.07	6.11 ± 0.09** ^c
14	5.90 ± 0.22	6.08 ± 0.28	6.32 ± 0.18** ^c
15		5.43 ± 0.02	<4.5** ^c
64		9.44 ± 0.01	9.44 ± 0.06*

^aDetermined by equilibrium competition binding with [³H]44 (2 nM) or [³H]64 (0.3 nM) at CHO-hM₂R cell homogenates; mean values ± SEM from at least three independent experiments (performed in triplicate). ^bDetermined by equilibrium competition binding with [³H]5 (0.2 nM) at live CHO-hM₂R cells; mean ± SEM from at least three independent experiments (performed in triplicate). ^cReported by Pegoli et al.²³

250 × 21 mm (Macherey-Nagel, Düren, Germany) was used as the stationary phase at a flow rate of 15 mL/min. Mixtures of acetonitrile and 0.1% aq TFA were used as the mobile phase, and a detection wavelength of 220 nm was used throughout. Lyophilization of the collected fractions was performed with an Alpha 2-4 LD apparatus (Martin Christ, Osterode am Harz, Germany). Except for compound **54**, analytical HPLC analysis (purity control) was performed on a system from Merck-Hitachi (Hitachi, Düsseldorf, Germany) composed of a L-6200-A pump, an AS-2000A autosampler, a L-4000A UV detector, and a D-6000 interface. A Kinetex-XB C18 column, 5 μm, 250

mm × 4.6 mm (Phenomenex, Aschaffenburg, Germany) was used as the stationary phase at a flow rate of 0.8 mL/min. Mixtures of acetonitrile (A) and 0.1% aq TFA (B) were used as the mobile phase (degassed by helium purging). The following linear gradient was applied: 0–30 min: A/B 5:95–85:15, 30–32 min: 85:15–95:5, and 32–40 min: 95:5. Detection was performed at 220 nm throughout. The oven temperature was 30 °C. Analytical HPLC analysis of **54** was performed on a system from Thermo Separation Products composed of a SN400 controller, a P4000 pump, a degasser (Degassex DG-4400, Phenomenex), an AS3000 autosampler, and a Spectra Focus ultraviolet–visible detector. A Eurospher-100 C18 column, 5 μm, 250 × 4 mm (Knauer, Berlin, Germany) served as reversed-phase (RP) column at a flow rate of 0.8 mL/min. Mixtures of acetonitrile (A) and 0.05% aq TFA (B) were used as the mobile phase (degassed by helium purging). The oven temperature was set to 30 °C, and detection was performed at 220 nm. The following linear gradient was applied: 0–30 min: A/B 20:80–95:5 and 30–40 min: 95:5.

Annotation concerning the NMR spectra (¹H, ¹³C) of the dibenzodiazepinone derivatives (**34**, **35**, **38**, **39**, **43**, **44**, **46**, **48**, **50**, **52**, **58–61**, **63**, **64**, **66**, **69**, and **72**): due to a slow rotation about the exocyclic amide group on the NMR time scale, two isomers (ratios provided in the experimental protocols) were evident in the ¹H- and ¹³C-NMR spectra.

4.2. Compound Characterization. Nondescribed intermediate compounds were characterized by ¹H- and ¹³C-NMR spectroscopy, HRMS, and melting point (if applicable). Target compounds were characterized by ¹H- and ¹³C-NMR spectroscopy, HRMS, and RP-HPLC analysis. In addition, compounds **44** and **64** were analyzed by IR spectroscopy. Purities determined by analytical RP-HPLC amounted to >95%.

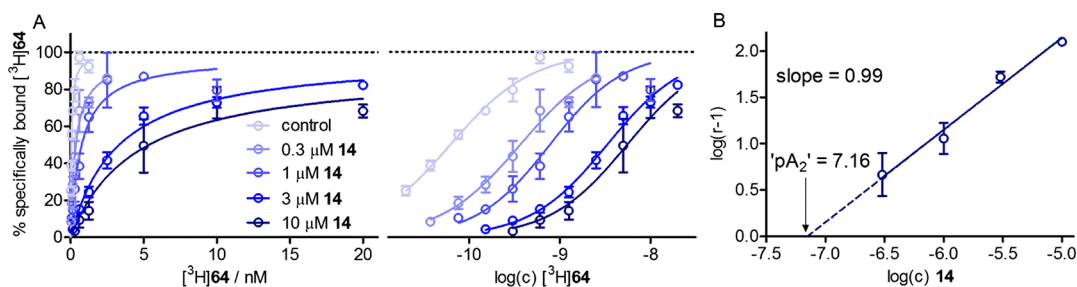


Figure 7. Effect of allosteric M_2R modulator **14** on the saturation binding of $[^3H]64$ determined at CHO-h M_2R cell homogenates at 22 °C. (A) Isotherms of specific radioligand binding plotted in the linear and semilogarithmic scale. The presence of compound **14** led to a rightward shift of the saturation isotherms of $[^3H]64$. (B) “Schild” regression resulting from the rightward shifts (ΔpK_d) of the saturation isotherms [$\log(r - 1)$ plotted vs $\log(\text{concentration } 14)$, where $r = 10^{\Delta pK_d}$]. The slope of the linear Schild regression was not different from unity [$P > 0.5$, based on the slope mean value \pm SEM (0.99 ± 0.15) from three sets of independent saturation-binding experiments (performed in triplicate)], suggesting a competitive interaction between $[^3H]64$ and **14**. Data represent mean values \pm SEM from three independent experiments (each performed in triplicate).

4.3. Investigation of the Chemical Stability. The chemical stability of **44** and **64** was investigated in PBS (pH 7.4) at 22 ± 1 °C. The incubation was started by addition of 10 mM solution of the compounds in dimethylsulfoxide (1 μ L) to PBS (99 μ L) to give a final concentration of 100 μ M. After 0, 12, and 48 h, an aliquot (20 μ L) of the solution was taken and added to acetonitrile/0.04% aq TFA (1:9 v/v) (20 μ L). An aliquot (20 μ L) of the resulting solution was analyzed by RP-HPLC using a system from Agilent Technologies (composed of a 1290 Infinity binary pump equipped with a degasser, a 1290 Infinity autosampler, a 1290 Infinity thermostated column compartment, a 1260 Infinity diode array detector, and a 1260 Infinity fluorescence detector). A Kinetex-XB C18 column, 2.6 μ m, 100 \times 3 mm (Phenomenex) served as the stationary phase at a flow rate of 0.5 mL/min. The following linear gradient was applied: 0–20 min: acetonitrile/0.04% aq TFA 10:90–68:32, 20–22 min: 68:32–95:5, and 22–28 min: 95:5. The detection wavelength was set to 220 nm.

4.4. Cell Culture and Preparation of Cell Homogenates. The culture conditions of CHO-K9 cells, stably transfected with the human muscarinic receptors M_1 – M_5 (obtained from Missouri S&T cDNA Resource Center; Rolla, MO), and the preparation of CHO-h M_2R cell homogenates are described elsewhere.²³

4.5. IP1 Accumulation Assay. The IP1 accumulation assay was performed as described elsewhere.²³

4.6. Radioligand Binding. Equilibrium competition-binding experiments with $[^3H]5$ were performed at intact CHO-h M_xR cells ($x = 1$ – 5) as described previously,²² but the total volume per well was 200 μ L, that is, in the case of total binding, the wells were filled with 180 μ L of L15 medium followed by addition of L15 medium (20 μ L) containing $[^3H]5$ (10-fold concentrated). To determine the unspecific binding and the effect of a compound of interest on the equilibrium binding $[^3H]5$, the wells were filled with 160 μ L of L15 medium followed by addition of L15 medium (20 μ L) containing **6** or the compound of interest (10-fold concentrated) and L15 medium (20 μ L) containing $[^3H]5$ (10-fold concentrated).

Saturation binding with $[^3H]44$ and $[^3H]64$ at intact CHO-h M_2R cells was performed in the same manner as saturation-binding experiments with $[^3H]5$ ²² with minor modifications: unspecific binding was determined in the presence of **6** (500-fold excess to $[^3H]44$ or $[^3H]64$), and the incubation period was 2 h.

Saturation and equilibrium competition-binding experiments with $[^3H]44$ and $[^3H]64$ at CHO-h M_2R cell homogenates were

performed according to the procedure described for saturation and competition-binding experiments with $[^3H]19$ at CHO-h M_2R cell homogenates,²³ using a total volume per well of 200 instead of 100 μ L. The total amount of soluble protein per well was between 19 and 43 μ g. In the case of competition-binding experiments, the radioligand concentration was 2.0 and 0.3 nM, respectively. To keep the total volume per well at 200 μ L in the case of saturation-binding experiments performed with $[^3H]64$ in the presence of **14**, the addition of L15 medium (20 μ L) containing **14** (10-fold concentrated) was compensated by an equivalent reduction in the volume of L15 medium added to the wells.

M_2R association experiments with $[^3H]44$ and $[^3H]64$ were performed at CHO-h M_2R cell homogenates essentially using the procedure described for saturation-binding experiments with $[^3H]19$ at CHO-h M_2R cell homogenates.²³ The radioligand concentration was 2 and 0.6 nM, respectively. The incubation was started in reversed order after different periods of time (120–1 min). After last addition of the radioligand, homogenates were collected on filter mats using the Harvester. Unspecific binding was determined in the presence of **6** (500-fold excess to the radioligand). For M_2R dissociation experiments with $[^3H]44$ and $[^3H]64$, performed at CHO-h M_2R cell homogenates, the procedure was essentially the same as for saturation-binding experiments with $[^3H]19$ at CHO-h M_2R cell homogenates.²³ The preincubation (60 min) of the cell homogenates with the radioligand ($[^3H]44$: 4 nM, $[^3H]64$: 0.6 nM) was started in reversed order after different periods of time ($[^3H]44$: between 180 and 1 min and $[^3H]64$: between 150 and 1 min) by addition of L15 medium (10 μ L) containing the radioligand (10-fold concentrated) to the wells preloaded with L15 medium (80 μ L) and cell homogenates (10 μ L). The dissociation was started by addition of 10 μ L of L15 medium containing **6** (40 and 6 μ M, respectively) and was stopped by collection and washing of the homogenates using the harvester. To determine unspecific binding, **6** (1000-fold excess to the radioligand) was added during the preincubation step.

4.7. Data Processing. Retention (capacity) factors were calculated from retention times (t_R) according to $k = (t_R - t_0)/t_0$ (t_0 = dead time). Data from the IP1 accumulation assay and radioligand-binding assays [saturation binding (including Schild-like analysis), association and dissociation kinetics, and equilibrium competition binding] were processed as described previously.²³ Statistical significance (curve slopes) was assessed by a t -test (one-sample, two-tailed). Propagated errors were calculated according to the Gaussian law of errors.

■ ASSOCIATED CONTENT

Supporting Information

The Supporting Information is available free of charge on the ACS Publications website at DOI: 10.1021/acsomega.7b01085.

Description of the synthesis of intermediates 20, 21, 23, 26, 30, 32, 33, 36, 37, 40, 42, 45, 47, 49, 53, 55–57, 62, 65, 68, and 71; experimental protocols for the synthesis and analytical data of compounds 20–23, 25, 26–39, 43–57, 58–72, 75–77, 79–81, 83, 84, 86, 87, 89, 90, 92, 93, 95–97, 100–104, 108–110, 114–116, 119, 121, 122, and 124; experimental protocol for the synthesis of the radioligands [³H]44 and [³H]64; ¹H-NMR and ¹³C-NMR spectra of compounds 22, 25, 27–29, 31, 34, 35, 38, 39, 43, 44, 46, 48, 50–52, 55, 58–61, 63, 64, 66, 67, 69, 70, and 72; RP-HPLC chromatograms of compounds 22, 25, 27–29, 31, 34, 35, 38, 39, 43, 44, 46, 48, 50–52, 55, 58–61, 63, 64, 66, 67, 69, 70, and 72 (PDF)

■ AUTHOR INFORMATION

Corresponding Author

*E-mail: max.keller@ur.de. Phone: (+49)941-9433329. Fax: (+49)941-9434820 (M.K.).

ORCID

Peter Gmeiner: 0000-0002-4127-197X

Max Keller: 0000-0002-8095-8627

Present Addresses

[§]HitGen, F7-10, Building B3, Tianfu Life Science Park 88 South Keyuan Road, Chengdu, 610041, China (X.S.).

^{||}Institute of Organic Chemistry, Faculty of Chemistry and Pharmacy, University of Regensburg, Universitätsstr. 31, D-93053 Regensburg, Germany (J.M.).

Notes

The authors declare no competing financial interest.

■ ACKNOWLEDGMENTS

The authors thank Brigitte Wenzl, Maria Beer-Krön, Dita Fritsch, and Susanne Bollwein for excellent technical assistance. The authors also thank Armin Buschauer for providing laboratory equipment and for helpful suggestions. This work was funded by the Graduate Training Program (Graduiertenkolleg) GRK1910 of the Deutsche Forschungsgemeinschaft (DFG) and by the China Scholarship Council (CSC).

■ ABBREVIATIONS

ACh, acetylcholine; Boc, *tert*-butoxycarbonyl; B_{max} , maximum number of binding sites; brs, broad singlet; CH₂Cl₂, dichloromethane; MeCN, acetonitrile; CHO-cells, Chinese hamster ovary cells; DCC, *N,N'*-dicyclohexylcarbodiimide; DIPEA, diisopropylethylamine; DMAP, 4-dimethylaminopyridine; dpm, disintegrations per minute; EtOAc, ethylacetate; GPCR, G-protein coupled receptor; HOBt, 1-hydroxybenzotriazole hydrate; IPI, inositol monophosphate; k , retention (or capacity) factor (HPLC); K_D , dissociation constant obtained from a saturation binding experiment; K_i , dissociation constant obtained from a competition binding experiment; k_{obs} , observed rate constant; k_{off} , dissociation rate constant; k_{on} , association rate constant; MR, muscarinic receptor; M_xR, muscarinic M_x ($x = 1–5$) receptor; PBS, phosphate buffered saline; pK_b , negative logarithm of the K_b (dissociation constant obtained from a functional assay (inhibition of the effect elicited by an agonist)) in M; pK_i , negative logarithm of the K_i in M; SEM, standard

error of the mean; TBTU, 2-(1*H*-benzotriazole-1-yl)-1,1,3,3-tetramethylammonium; TFA, trifluoroacetic acid; t_R , retention time

■ REFERENCES

- (1) Hammer, R.; Berrie, C. P.; Birdsall, N. J. M.; Burgen, A. S. V.; Hulme, E. C. Pirenzepine distinguishes between different subclasses of muscarinic receptors. *Nature* **1980**, *283*, 90–92.
- (2) Bonner, T.; Buckley, N.; Young, A.; Brann, M. Identification of a family of muscarinic acetylcholine receptor genes. *Science* **1987**, *237*, 527–532.
- (3) Caulfield, M. P. Muscarinic receptors—characterization, coupling and function. *Pharmacol. Ther.* **1993**, *58*, 319–379.
- (4) Caulfield, M. P.; Birdsall, N. J. International Union of Pharmacology. XVII. Classification of muscarinic acetylcholine receptors. *Pharmacol. Rev.* **1998**, *50*, 279–290.
- (5) Lanzafame, A. A.; Christopoulos, A.; Mitchelson, F. Cellular Signaling Mechanisms for Muscarinic Acetylcholine Receptors. *Recept. Channels* **2003**, *9*, 241–260.
- (6) Dean, B.; Bymaster, F.; Scarr, E. Muscarinic receptors in schizophrenia. *Curr. Mol. Med.* **2003**, *3*, 419–426.
- (7) Clader, J.; Wang, Y. Muscarinic receptor agonists and antagonists in the treatment of Alzheimer's disease. *Curr. Pharm. Des.* **2005**, *11*, 3353–3361.
- (8) Haga, K.; Kruse, A. C.; Asada, H.; Yurugi-Kobayashi, T.; Shiroishi, M.; Zhang, C.; Weis, W. I.; Okada, T.; Kobilka, B. K.; Haga, T.; Kobayashi, T. Structure of the human M₂ muscarinic acetylcholine receptor bound to an antagonist. *Nature* **2012**, *482*, 547–551.
- (9) Kruse, A. C.; Hu, J.; Pan, A. C.; Arlow, D. H.; Rosenbaum, D. M.; Rosemond, E.; Green, H. F.; Liu, T.; Chae, P. S.; Dror, R. O.; Shaw, D. E.; Weis, W. I.; Wess, J.; Kobilka, B. K. Structure and dynamics of the M₃ muscarinic acetylcholine receptor. *Nature* **2012**, *482*, 552–556.
- (10) Thal, D. M.; Sun, B.; Feng, D.; Nawaratne, V.; Leach, K.; Felder, C. C.; Bures, M. G.; Evans, D. A.; Weis, W. I.; Bachhawat, P.; Kobilka, T. S.; Sexton, P. M.; Kobilka, B. K.; Christopoulos, A. Crystal structures of the M₁ and M₄ muscarinic acetylcholine receptors. *Nature* **2016**, *531*, 335–340.
- (11) Eglén, R. M.; Choppin, A.; Watson, N. Therapeutic opportunities from muscarinic receptor research. *Trends Pharmacol. Sci.* **2001**, *22*, 409–414.
- (12) Mohr, K.; Tränkle, C.; Holzgrabe, U. Structure/activity relationships of M₂ muscarinic allosteric modulators. *Recept. Channels* **2003**, *9*, 229–240.
- (13) Voigtländer, U.; Jöhren, K.; Mohr, M.; Raasch, A.; Tränkle, C.; Buller, S.; Ellis, J.; Höltje, H.-D.; Mohr, K. Allosteric site on muscarinic acetylcholine receptors: identification of two amino acids in the muscarinic M₂ receptor that account entirely for the M₂/M₅ subtype selectivities of some structurally diverse allosteric ligands in N-methylscopolamine-occupied receptors. *Mol. Pharmacol.* **2003**, *64*, 21–31.
- (14) Wess, J. Allosteric binding sites on muscarinic acetylcholine receptors. *Mol. Pharmacol.* **2005**, *68*, 1506–1509.
- (15) Presland, J. Identifying novel modulators of G protein-coupled receptors via interaction at allosteric sites. *Curr. Opin. Drug Discovery Dev.* **2005**, *8*, 567–576.
- (16) Conn, P. J.; Christopoulos, A.; Lindsley, C. W. Allosteric modulators of GPCRs: a novel approach for the treatment of CNS disorders. *Nat. Rev. Drug Discovery* **2009**, *8*, 41–54.
- (17) Kruse, A. C.; Ring, A. M.; Manglik, A.; Hu, J.; Hu, K.; Eitel, K.; Hübner, H.; Pardon, E.; Valant, C.; Sexton, P. M. Activation and allosteric modulation of a muscarinic acetylcholine receptor. *Nature* **2013**, *504*, 101–106.
- (18) Lüllmann, H.; Ohnesorge, F. K.; Schauwecker, G.-C.; Wassermann, O. Inhibition of the actions of carbachol and DFP on guinea pig isolated atria by alkane-bis-ammonium compounds. *Eur. J. Pharmacol.* **1969**, *6*, 241–247.

- (19) Mohr, K.; Tränkle, C.; Kostenis, E.; Barocelli, E.; De Amici, M.; Holzgrabe, U. Rational design of dualsteric GPCR ligands: quests and promise. *Br. J. Pharmacol.* **2010**, *159*, 997–1008.
- (20) Clark, A. L.; Mitchelson, F. The inhibitory effect of gallamine on muscarinic receptors. *Br. J. Pharmacol.* **1976**, *58*, 323–331.
- (21) Tränkle, C.; Andresen, I.; Lambrecht, G.; Mohr, K. M₂ receptor binding of the selective antagonist AF-DX 384: possible involvement of the common allosteric site. *Mol. Pharmacol.* **1998**, *53*, 304–312.
- (22) Keller, M.; Tränkle, C.; She, X.; Pegoli, A.; Bernhardt, G.; Buschauer, A.; Read, R. W. M₂ Subtype preferring dibenzodiazepinone-type muscarinic receptor ligands: Effect of chemical homodimerization on orthosteric (and allosteric?) binding. *Bioorg. Med. Chem.* **2015**, *23*, 3970–3990.
- (23) Pegoli, A.; She, X.; Wifling, D.; Hübner, H.; Bernhardt, G.; Gmeiner, P.; Keller, M. Radiolabeled Dibenzodiazepinone-Type Antagonists Give Evidence of Dualsteric Binding at the M₂ Muscarinic Acetylcholine Receptor. *J. Med. Chem.* **2017**, *60*, 3314–3334.
- (24) Croy, C. H.; Schober, D. A.; Xiao, H.; Quets, A.; Christopoulos, A.; Felder, C. C. Characterization of the novel positive allosteric modulator, LY2119620, at the muscarinic M₂ and M₄ receptors. *Mol. Pharmacol.* **2014**, *86*, 106–115.
- (25) Schober, D. A.; Croy, C. H.; Xiao, H.; Christopoulos, A.; Felder, C. C. Development of a Radioligand, [³H]LY2119620, to Probe the Human M₂ and M₄ Muscarinic Receptor Allosteric Binding Sites. *Mol. Pharmacol.* **2014**, *86*, 116–123.
- (26) Shonberg, J.; Scammells, P. J.; Capuano, B. Design strategies for bivalent ligands targeting GPCRs. *ChemMedChem* **2011**, *6*, 963–974.
- (27) Berque-Bestel, I.; Lezoualc'h, F.; Jockers, R. Bivalent ligands as specific pharmacological tools for G protein-coupled receptor dimers. *Curr. Drug Discovery Technol.* **2008**, *5*, 312–318.
- (28) Bhushan, R. G.; Sharma, S. K.; Xie, Z.; Daniels, D. J.; Portoghese, P. S. A bivalent ligand (KDN-21) reveals spinal δ and κ opioid receptors are organized as heterodimers that give rise to δ_1 and κ_2 phenotypes. Selective targeting of δ - κ heterodimers. *J. Med. Chem.* **2004**, *47*, 2969–2972.
- (29) Birnkammer, T.; Spickenreither, A.; Brunskole, I.; Lopuch, M.; Kagermeier, N.; Bernhardt, G.; Dove, S.; Seifert, R.; Elz, S.; Buschauer, A. The bivalent ligand approach leads to highly potent and selective acylguanidine-type histamine H₂ receptor agonists. *J. Med. Chem.* **2012**, *55*, 1147–1160.
- (30) Kagermeier, N.; Werner, K.; Keller, M.; Baumeister, P.; Bernhardt, G.; Seifert, R.; Buschauer, A. Dimeric carbamoylguanidine-type histamine H₂ receptor ligands: A new class of potent and selective agonists. *Bioorg. Med. Chem.* **2015**, *23*, 3957–3969.
- (31) Huber, D.; Hübner, H.; Gmeiner, P. 1,1'-Disubstituted ferrocenes as molecular hinges in mono- and bivalent dopamine receptor ligands. *J. Med. Chem.* **2009**, *52*, 6860–6870.
- (32) Kühhorn, J.; Hübner, H.; Gmeiner, P. Bivalent dopamine D₂ receptor ligands: synthesis and binding properties. *J. Med. Chem.* **2011**, *54*, 4896–4903.
- (33) Soriano, A.; Ventura, R.; Molero, A.; Hoen, R.; Casadó, V.; Cortés, A.; Fanelli, F.; Albericio, F.; Lluís, C.; Franco, R.; Royo, M. Adenosine A₂A receptor-antagonist/dopamine D₂ receptor-agonist bivalent ligands as pharmacological tools to detect A₂A-D₂ receptor heteromers. *J. Med. Chem.* **2009**, *52*, 5590–5602.
- (34) Jacobson, K. A.; Xie, R.; Young, L.; Chang, L.; Liang, B. T. A novel pharmacological approach to treating cardiac ischemia binary conjugates of A₁ and A₃ adenosine receptor agonists. *J. Biol. Chem.* **2000**, *275*, 30272–30279.
- (35) Hausler, N. E.; Devine, S. M.; McRobb, F. M.; Warfe, L.; Pouton, C. W.; Haynes, J. M.; Bottle, S. E.; White, P. J.; Scammells, P. J. Synthesis and pharmacological evaluation of dual acting antioxidant A₂A adenosine receptor agonists. *J. Med. Chem.* **2012**, *55*, 3521–3534.
- (36) Weiss, S.; Keller, M.; Bernhardt, G.; Buschauer, A.; König, B. Modular synthesis of non-peptidic bivalent NPY Y₁ receptor antagonists. *Bioorg. Med. Chem.* **2008**, *16*, 9858–9866.
- (37) Keller, M.; Teng, S.; Bernhardt, G.; Buschauer, A. Bivalent Argininamide-Type Neuropeptide Y Y₁ Antagonists Do Not Support the Hypothesis of Receptor Dimerisation. *ChemMedChem* **2009**, *4*, 1733–1745.
- (38) Keller, M.; Kaske, M.; Holzammer, T.; Bernhardt, G.; Buschauer, A. Dimeric argininamide-type neuropeptide Y receptor antagonists: chiral discrimination between Y₁ and Y₄ receptors. *Bioorg. Med. Chem.* **2013**, *21*, 6303–6322.
- (39) Davie, B. J.; Christopoulos, A.; Scammells, P. J. Development of M₁ mAChR allosteric and bitopic ligands: prospective therapeutics for the treatment of cognitive deficits. *ACS Chem. Neurosci.* **2013**, *4*, 1026–1048.
- (40) Valant, C.; Lane, J. R.; Sexton, P. M.; Christopoulos, A. The best of both worlds? Bitopic orthosteric/allosteric ligands of G protein-coupled receptors. *Annu. Rev. Pharmacol. Toxicol.* **2012**, *52*, 153–178.
- (41) Antony, J.; Kellershohn, K.; Mohr-Andra, M.; Kebig, A.; Prilla, S.; Muth, M.; Heller, E.; Disingrini, T.; Dallanocce, C.; Bertoni, S.; Schrobang, J.; Tränkle, C.; Kostenis, E.; Christopoulos, A.; Holtje, H.-D.; Barocelli, E.; De Amici, M.; Holzgrabe, U.; Mohr, K. Dualsteric GPCR targeting: a novel route to binding and signaling pathway selectivity. *FASEB J.* **2009**, *23*, 442–450.
- (42) Lane, J. R.; Sexton, P. M.; Christopoulos, A. Bridging the gap: bitopic ligands of G-protein-coupled receptors. *Trends Pharmacol. Sci.* **2013**, *34*, 59–66.
- (43) Disingrini, T.; Muth, M.; Dallanocce, C.; Barocelli, E.; Bertoni, S.; Kellershohn, K.; Mohr, K.; De Amici, M.; Holzgrabe, U. Design, synthesis, and action of oxotremorine-related hybrid-type allosteric modulators of muscarinic acetylcholine receptors. *J. Med. Chem.* **2006**, *49*, 366–372.
- (44) Steinfeld, T.; Mammen, M.; Smith, J. A. M.; Wilson, R. D.; Jasper, J. R. A novel multivalent ligand that bridges the allosteric and orthosteric binding sites of the M₂ muscarinic receptor. *Mol. Pharmacol.* **2007**, *72*, 291–302.
- (45) Dörje, F.; Wess, J.; Lambrecht, G.; Tacke, R.; Mutschler, E.; Brann, M. R. Antagonist binding profiles of five cloned human muscarinic receptor subtypes. *J. Pharmacol. Exp. Ther.* **1991**, *256*, 727–733.
- (46) Gitler, M. S.; Reba, R. C.; Cohen, V. I.; Rzeszutarski, W. J.; Baumgold, J. A novel m2-selective muscarinic antagonist: binding characteristics and autoradiographic distribution in rat brain. *Brain Res.* **1992**, *582*, 253–260.
- (47) Mohr, M.; Heller, E.; Ataie, A.; Mohr, K.; Holzgrabe, U. Development of a new type of allosteric modulator of muscarinic receptors: hybrids of the antagonist AF-DX 384 and the hexamethonium derivative W84. *J. Med. Chem.* **2004**, *47*, 3324–3327.
- (48) Holzgrabe, U.; De Amici, M.; Mohr, K. Allosteric modulators and selective agonists of muscarinic receptors. *J. Mol. Neurosci.* **2006**, *30*, 165–167.
- (49) Shekhar, A.; Potter, W. Z.; Lightfoot, J.; Lienemann, J.; Dubé, S.; Mallinckrodt, C.; Bymaster, F. P.; McKinzie, D. L.; Felder, C. C. Selective muscarinic receptor agonist xanomeline as a novel treatment approach for schizophrenia. *Am. J. Psychiatry* **2008**, *165*, 1033–1039.
- (50) Bridges, T. M.; Brady, A. E.; Kennedy, J. P.; Daniels, R. N.; Miller, N. R.; Kim, K.; Breining, M. L.; Gentry, P. R.; Brogan, J. T.; Jones, C. K.; Conn, P. J.; Lindsley, C. W. Synthesis and SAR of analogues of the M₁ allosteric agonist TBPB. Part I: Exploration of alternative benzyl and privileged structure moieties. *Bioorg. Med. Chem. Lett.* **2008**, *18*, 5439–5442.
- (51) Miller, N. R.; Daniels, R. N.; Bridges, T. M.; Brady, A. E.; Conn, P. J.; Lindsley, C. W. Synthesis and SAR of analogs of the M₁ allosteric agonist TBPB. Part II: Amides, sulfonamides and ureas—The effect of capping the distal basic piperidine nitrogen. *Bioorg. Med. Chem. Lett.* **2008**, *18*, 5443–5447.
- (52) Jones, C. K.; Brady, A. E.; Davis, A. A.; Xiang, Z.; Buser, M.; Tantawy, M. N.; Kane, A. S.; Bridges, T. M.; Kennedy, J. P.; Bradley, S. R. Novel selective allosteric activator of the M₁ muscarinic acetylcholine receptor regulates amyloid processing and produces antipsychotic-like activity in rats. *J. Neurosci.* **2008**, *28*, 10422–10433.
- (53) Keov, P.; Valant, C.; Devine, S. M.; Lane, J. R.; Scammells, P. J.; Sexton, P. M.; Christopoulos, A. Reverse engineering of the selective agonist TBPB unveils both orthosteric and allosteric modes of action

at the M_1 muscarinic acetylcholine receptor. *Mol. Pharmacol.* **2013**, *84*, 425–437.

(54) Avlani, V. A.; Langmead, C. J.; Guida, E.; Wood, M. D.; Tehan, B. G.; Herdon, H. J.; Watson, J. M.; Sexton, P. M.; Christopoulos, A. Orthosteric and allosteric modes of interaction of novel selective agonists of the M_1 muscarinic acetylcholine receptor. *Mol. Pharmacol.* **2010**, *78*, 94–104.

(55) Huang, F.; Buchwald, P.; Browne, C. E.; Farag, H. H.; Wu, W.-M.; Ji, F.; Hochhaus, G.; Bodor, N. Receptor binding studies of soft anticholinergic agents. *AAPS PharmSci* **2001**, *3*, 44–56.

(56) Maggio, R.; Barbier, P.; Bolognesi, M. L.; Minarini, A.; Tedeschi, D.; Melchiorre, C. Binding profile of the selective muscarinic receptor antagonist tripitramine. *Eur. J. Pharmacol.* **1994**, *268*, 459–462.

(57) Copeland, R. A. Conformational adaptation in drug–target interactions and residence time. *Future Med. Chem.* **2011**, *3*, 1491–1501.

(58) Vauquelin, G. Simplified models for heterobivalent ligand binding: when are they applicable and which are the factors that affect their target residence time. *Naunyn-Schmiedeberg's Arch. Pharmacol.* **2013**, *386*, 949–962.

(59) Tränkle, C.; Weyand, O.; Voigtländer, U.; Mynett, A.; Lazareno, S.; Birdsall, N. J. M.; Mohr, K. Interactions of orthosteric and allosteric ligands with [3 H]dimethyl-W84 at the common allosteric site of muscarinic M_2 receptors. *Mol. Pharmacol.* **2003**, *64*, 180–190.

(60) Keller, M.; Pop, N.; Hutzler, C.; Beck-Sickingler, A. G.; Bernhardt, G.; Buschauer, A. Guanidine–acylguanidine bioisosteric approach in the design of radioligands: synthesis of a tritium-labeled N^G -propionylargininamide ([3 H]-UR-MK114) as a highly potent and selective neuropeptide Y Y1 receptor antagonist. *J. Med. Chem.* **2008**, *51*, 8168–8172.

(61) Kane, B. E.; Grant, M. K. O.; El-Fakahany, E. E.; Ferguson, D. M. Synthesis and evaluation of xanomeline analogs—Probing the wash-resistant phenomenon at the M_1 muscarinic acetylcholine receptor. *Bioorg. Med. Chem.* **2008**, *16*, 1376–1392.

(62) Cohen, V. I.; Baumgold, J.; Jin, B.; De la Cruz, R.; Rzeszutarski, W. J.; Reba, R. C. Synthesis and structure-activity relationship of some 5-[[[(dialkylamino)alkyl]-1-piperidiny]acetyl]-10,11-dihydro-5H-dibenzo[b,e][1,4]diazepin-11-ones as M_2 -selective antimuscarinics. *J. Med. Chem.* **1993**, *36*, 162–165.